ISSN 0021-3640, JETP Letters, 2018, Vol. 108, No. 6, pp. 356–363. © Pleiades Publishing, Inc., 2018.
Original Russian Text © S.I. Popel, A.P. Golub', A.V. Zakharov, L.M. Zelenyi, A.A. Berezhnoy, E.S. Zubko, M. Iten, R. Lena, S. Sposetti, Yu.I. Velikodsky, A.A. Tereshchenko, B. Atamaniuk, 2018, published in Pis'ma v Zhurnal Eksperimental'noi i Teoreticheskoi Fiziki, 2018, Vol. 108, No. 6, pp. 379–387.

ASTROPHYSICS AND COSMOLOGY

Formation of Dusty Plasma Clouds at Meteoroid Impact on the Surface of the Moon

S. I. Popel[a, b, *], A. P. Golub'[a], A. V. Zakharov[a], L. M. Zelenyi[a, c], A. A. Berezhnoy[d], E. S. Zubko[e], M. Iten[f], R. Lena[g], S. Sposetti[h], Yu. I. Velikodsky[i], A. A. Tereshchenko[i], and B. Atamaniuk[j]

[a] *Space Research Institute, Russian Academy of Sciences, Moscow, 117997 Russia*
[b] *National Research University Higher School of Economics, Moscow, 101000 Russia*
[c] *Moscow Institute of Physics and Technology (State University), Dolgoprudnyi, Moscow region, 141700 Russia*
[d] *Sternberg Astronomical Institute, Moscow State University, Moscow, 119234 Russia*
[e] *Far Eastern Federal University, Vladivostok, 690091 Russia*
[f] *Garden Observatory, CH-6596 Gordola, Switzerland*
[g] *Geologic Lunar Research (GLR) Group, 00137 Rome, Italy*
[h] *Gnosca Observatory, CH-6525 Gnosca, Switzerland*
[i] *National Aviation University, Kyiv, 03058 Ukraine*
[j] *Space Research Centre, Polish Academy of Sciences, 00-716 Warsaw, Poland*
**e-mail: popel@iki.rssi.ru*

Received August 6, 2018; in final form, August 17, 2018

The nature of two dusty plasma clouds appearing because of the impact of a meteoroid on the surface of the Moon has been discussed. It has been shown that one of the clouds is formed by particles (or fragments) of regolith ejected into free space by a shock wave induced by the meteoroid impact on the surface of the Moon and the second cloud is formed by solidified melt droplets. The main characteristics of these clouds, including the cloud expansion rates, the characteristic sizes of particles in both clouds, and the concentrations and charges of particles, have been calculated. The calculated cloud expansion rates are in qualitative agreement with the observational data.

DOI: 10.1134/S0021364018180091

Dust and dusty plasma over the Moon are actively studied now [1–8]. The Luna-25, Luna-26, Luna-27, etc., missions are under preparation in Russia. The landers of the Luna-25 and Luna-27 spacecrafts will assumingly be equipped with instruments for the study of the properties of dust and dusty plasma over the surface of the Moon [9–11]. The NASA mission LADEE (Lunar Atmosphere and Dust Environment Explorer) [12, 13] launched in 2013 studied the dusty plasma in a wide range of altitudes above the Moon by means of observations from orbit.

Important sources of dust over the surface of the Moon are meteoroid impacts, which result in the elevation of dust particles, in particular, to high altitudes (see, e.g., [14, 15]). Works [14, 15] concerned the situation where the density of dust particles over the Moon is determined by the flux of meteoroids colliding with the surface of the Moon. However, single impacts of sufficiently large meteoroids on the Moon also affect the state of a dusty plasma system. The effect of single impacts of large meteoroids on the possibility of formation of dust over the Moon was only estimated in [16] within the study of *transient atmospheres* formed near atmosphereless celestial bodies, in particular, the Moon. Correspondingly, the features of dusty plasma clouds formed at impacts of large meteoroids on the surface of the Moon were not discussed.

The observations of short-term optical flashes, seismic waves, and concentration of Na in the lunar exosphere usually indicate collisions of meteoroids with the Moon. The direct study of the properties of a dusty plasma cloud is usually impossible. However, at 21:35:22.871 (± 0.010 s) UT February 26, 2015, using a 125-mm refractor (Gordola, Switzerland) equipped with a Watec 902H2 Ultimate video camera, M. Iten detected an optical flash from a meteoroid impact on the dark part of the surface of the Moon near the terminator. The observation of the meteoroid impact on the dark part of the surface of the Moon near the terminator implies that this phenomenon is rare. However, this allowed detailed observations of the evolution of luminescence induced by the impact. Indeed, the flash from the meteoroid impact is characterized by thermal radiation, whereas luminescence observed in subsequent times is due to the scattering of solar light by dust particles rising over the surface of the

Moon because of the meteoroid impact. Luminescence associated with the scattering of solar light by dust particles can be reliably observed only when the meteoroid impact occurs on the dark part of the Moon near the terminator. Otherwise, either the illumination of the surface of the Moon hinders observation or solar light is not incident on dust particles rising over the Moon.

It is noteworthy that the monitoring of optical flashes on the Moon revealed several hundred lunar optical flashes induced by meteoroid impacts [17]. According to the statistics, the observation of impact-induced flashes and formed dusty plasma clouds near the lunar terminator could be expected. However, the observation of such flashes has not been reported. Thus, the formation of dusty plasma clouds after the incidence of a large meteoroid near the lunar terminator is considered for the first time in this work. Such phenomena have not yet been discussed. For this reason, the study of the parameters of formed dusty plasma clouds is topical in view of the possibility of observation of similar events in the near future.

Figure 1 shows photographs of the region where the flash occurs taken at 0.25 s before the flash and at 4, 8, 12, 16, and 20 s after the flash. It is seen in Fig. 1 that the luminescence region formed by the meteoroid impact expands. The luminescence picture shown in Fig. 1 is related to the dust distribution over the surface of the Moon after the meteoroid impact, and the information on the behavior of dust over the Moon can be obtained from photographs taken after the flash. All five photographs taken after the flash demonstrate a large expanding cloud. Beginning with 12th second, a small (slow) cloud is clearly seen in the form of a light spot at the point (0, 0). This cloud dominates in brightness already at the 20th second.

The aim of the further calculations are, first, to reveal a mechanism responsible for the formation of two dusty plasma clouds because of the impact of a sufficiently large meteoroid on the surface of the Moon and, second, to estimate the characteristics of the dusty plasma clouds. The method proposed in [18] to reconstruct the kinetic energy of an impactor from the maximum flash brightness makes it possible to estimate the range of possible kinetic energies of the meteoroid from 6×10^8 to 1.7×10^9 J. The calculations were performed for the impactor mass $m_i = 4.7$ kg and its velocity $u_i = 27$ km/s, which corresponds to the upper bound (1.7×10^9 J) of this range of possible kinetic energies. It was found that the use of the characteristics of the meteoroid corresponding to the lower bound of this range cannot explain the observation of two (fast large and slow small) dusty plasma clouds. Consequently, it is necessary to consider a sufficiently large fast meteoroid whose kinetic energy much higher than 6×10^8 J.

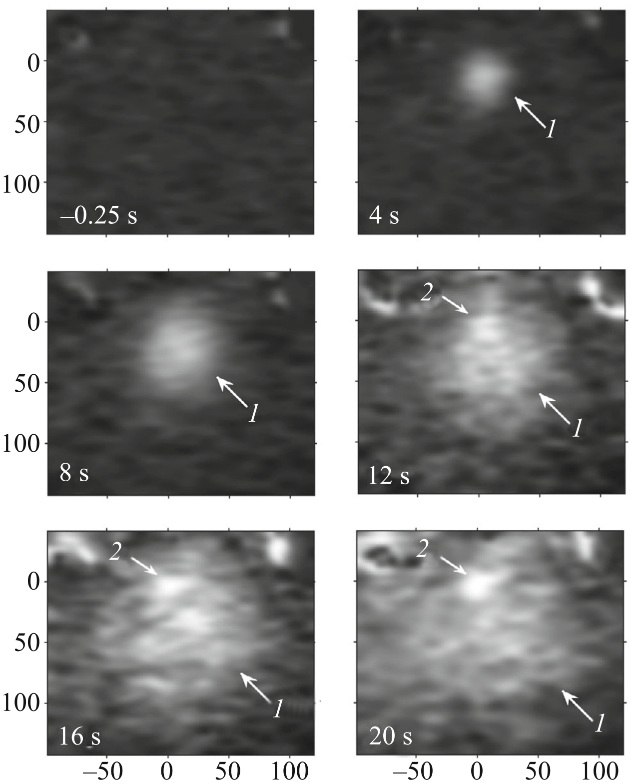

Fig. 1. Photographs of the region where the meteoroid collides at the point (0, 0) with the surface of the Moon taken at 0.25 s before the collision and at 4, 8, 12, 16, and 20 s after the collision. The axes present distances in kilometers. Arrows *1* and *2* indicate the fast large and slow small dust clouds, respectively.

The parameters used make it possible to assume [15] that the specific energy of the impactor $u_i^2/2$ is much higher than a value of 10 MJ/kg characteristic of the binding energy of atoms and molecules in the impactor and lunar regolith (which consists of fragments of lunar rocks and minerals whose sizes range from dust particles to several meters in diameter, glasses, lithified breccia, fragments of meteorites, etc.). In this case, the meteoroid impact on the surface of the Moon results in the strong compression and heating of the materials of the impactor and target. In view of a high pressure, a strong shock wave is formed and propagates with weakening from the epicenter of the meteoroidal explosion. Finally, the weakened shock wave is transformed to a linear acoustic wave.

The calculations were performed for the situation where the impactor consists of continuous gabbroid anorthosite, whereas the material of the target is porous gabbroid anorthosite. It is assumed that the densities of the impactor and target before the collision are $\rho_{i0} = 3$ g/cm^3 and $\rho_{t0} = 1.4$ g/cm^3, respectively. The radius of the impactor is $a_i = 7.2$ cm and the porosity of the target is $k = \rho_{i0}/\rho_{t0} = 2.14$. It is also assumed that the relation between the velocity of the strong shock wave $D_{\mathrm{i,t}}$ and the mass velocity u behind the shock front is linear: $D_{\mathrm{i,t}} = C_{\mathrm{i,t}} + S_{\mathrm{i,t}}u$. Here, the subscripts i and t specify the materials of the impactor and target, respectively; $C_{\mathrm{i}} = 7.71$ km/s; $S_{\mathrm{i}} = 1.05$; $C_{\mathrm{t}} = C_{\mathrm{i}}k/(1 + S_{\mathrm{i}}(k-1)) = 7.51$ km/s; and $S_{\mathrm{t}} = S_{\mathrm{i}}k/(1 + S_{\mathrm{i}}(k-1)) = 1.02$. The velocity of the shock wave and the mass velocity unambiguously determine the equation of state in terms of the well-known Hugoniot equations. The linear relation between these velocities usually describes experimental data fairly well (see [19]).

To determine the size distribution of dust particles in lunar regolith, we used data from [20] for sizes of dust particles from 20 to 500 μm. These data allow obtaining the distribution of dust particles in lunar regolith, which are in good agreement with the Kolmogorov distribution [4] for the probability $\Phi(L)$ of finding a particle of lunar regolith with the radius (characteristic size) smaller than L for the case of multiple fragmentation. This fact is in agreement with the conclusion made in [20] that the surface of the Moon is regolith evolving because of multiple fragmentation caused by meteoroid impacts. This Kolmogorov distribution is used in subsequent calculations.

The considered impact of a sufficiently large fast meteoroid on the surface of the Moon results in the formation of zones (cf. [14, 15]) of various processes around the equivalent center of the meteoroid explosion located at the depth

$$W_0 = \frac{2a_{\mathrm{i}}\rho_{\mathrm{i0}}\cos\theta}{\rho_{\mathrm{t0}}} \quad (1)$$

under the surface. Here, θ is the angle of incidence of the meteoroid on the surface of the Moon. These zones are the (I) material evaporation zone; (II) material melting zone; (III) zone of destruction of lunar regolith particles and their irreversible deformations; (IV) zone of nonlinear elastic deformation of regolith, where pressures in a nonlinear acoustic wave are below the dynamic elasticity limit; and (V) zone of linear elastic deformations of regolith, where the acoustic wave can be considered as linear. The boundaries of zones are parts of spheres whose center coincides with the equivalent center of the meteoroid explosion. In the considered situation and under the condition that the speed of sound in unperturbed regolith is c_0 = 300 m/s, the radii of the outer boundaries of zones I, II, III, and IV under the surface of the Moon are approximately $r_{\mathrm{I}} \approx 0.31u_{\mathrm{i}}^{2/3}a_{\mathrm{i}}$, $r_{\mathrm{II}} \approx 0.58u_{\mathrm{i}}^{2/3}a_{\mathrm{i}}$, $r_{\mathrm{III}} \approx 0.93u_{\mathrm{i}}^{2/3}a_{\mathrm{i}}$, and $r_{\mathrm{IV}} \approx 1.3u_{\mathrm{i}}^{2/3}a_{\mathrm{i}}$, where the velocity u_{i} is given in kilometers per second. The substitution of the radius of the impactor $a_{\mathrm{i}} = 7.2$ cm and its velocity $u_{\mathrm{i}} = 27$ km/s gives $r_{\mathrm{I}} = 20.1$ cm, $r_{\mathrm{II}} = 37.6$ cm, r_{III} = 60.3 cm, and $r_{\mathrm{IV}} = 84.3$ cm.

Zones III–V are sources of dust particles, which are regolith particles or their fragments, over the surface of the Moon. The greater part of dust escaping from the surface of the Moon owing to meteoroid impacts originates from zone V of linear elastic deformation of regolith. Indeed, the mass of dust particles from zone V rising over the surface of the Moon at altitudes above 10 m (1 km) is 80 (6) times larger than the mass of matter rising from other zones (I–IV) [15]. Zones I and II are sources of evaporated and melted material of the impactor and regolith. The material ejected by the shock wave into free space from the material melting zone II is a liquid decaying into fragments. Liquid material droplets are formed, solidify, and rise to altitudes of about 100 km and higher [15]. Rising over the surface of the Moon, both regolith particles (or their fragments) and melt droplets become charged because of the interaction, in particular, with electrons and ions of the solar wind, as well as with solar radiation. As a result, two dusty plasma clouds are formed: the first formed by regolith particles (or fragments) and the second formed by solidified melt droplets. These clouds have different characteristics, e.g., the expansion velocity, and, consequently, can be observed individually.

The velocity and amount of material rising over the surface of the Moon can be calculated for zone V of linear elastic deformations of regolith and material melting zone II. In fact, since the greater part of dust particles leaving the surface of the Moon because of meteoroid impacts originate from zone V, these calculations are sufficient to reveal the main characteristics of dusty plasma clouds.

In zone V of linear elastic deformations of regolith, fragments of lunar rock located in the surface layer with the depth (so-called spallation [15])

$$w = w_{\mathrm{c}} = 0.5c_0\tau_+, \quad \text{if} \quad r > r_{\mathrm{IV}}, \quad (2)$$

are separated from the surface of the Moon because of the interaction with a compression wave. Here, τ_+ is the time of the positive phase ($u_r > 0$) in the shock wave and u_r is the horizontal component of the mass velocity in the shock wave. To determine the depth of the spall layer in zones I–IV, we use the linear interpolation

$$w(r) = W_0 + \frac{w_{\mathrm{c}} - W_0}{r_{\mathrm{IV}}}r, \quad \text{if} \quad r \le r_{\mathrm{IV}}. \quad (3)$$

At $a_{\mathrm{i}} = 7.2$ cm and $u_{\mathrm{i}} = 27$ km/s, the depth of the spall layer in zone V is $w_{\mathrm{c}} = 38.9$ cm. When the shock wave propagates along the surface of the Moon from the epicenter of the meteoroid explosion, a rarefaction wave is formed in the surface layer and the vertical component u_z of the mass velocity appears behind the shock front. At $r > r_{\mathrm{IV}}$, $u_r = (1-1.5)u_z$ [21]. The calculations were performed at $u_r = u_z$ (cf. [14, 15]). Using expressions for the depth of the spall layer w and the size distribution of regolith particles on the surface of the Moon, one can find the amount and characteristic sizes of dust particles rising over the surface of the Moon per unit time because of the meteoroid impact.

The material ejected by the shock wave from the material melting zone II into free space is a liquid decaying into fragments. Equilibrium drops are formed when the volume occupied by vapor in the drop–vapor flux becomes comparable to the volume of the liquid [15]. The equilibrium radius of a drop (at $t \to \infty$) formed (owing to the meteoroid impact) in the material melting zone II has the form [22]

$$r_\infty = a_{\mathrm{dr}} = \left(\frac{15}{4}\frac{\sigma C_{\mathrm{D}}}{\rho_{\mathrm{d}} a}\right)^{1/2}. \quad (4)$$

Here, a_{dr} is the characteristic radius of the drop, σ is the surface tension of the liquid drop (the usual value for silicate particles is $\sigma \sim 0.3$ N/m), C_{D} is the drag coefficient at the motion of the drop in the vapor flow, ρ_{d} is the drop material density, a is the length of the acceleration vector $\mathbf{a} = -(1/\rho)\boldsymbol{\nabla} P$, ρ is the density of the drop–vapor mixture, and $\boldsymbol{\nabla} P$is the gradient of the pressure P.

Calculating the gradient of the pressure with the parameters of the shock wave appearing because of the impact of a fast meteoroid, setting $C_{\mathrm{D}} = 1$ (see [22]), $\rho_{\mathrm{d}} = 3$ g/cm^3, $\sigma = 0.3$ N/m, and taking into account that most of the melt drops rise from the part of zone II close to the outer boundary of this zone, we obtain the characteristic radius of the drop

$$a_{\mathrm{dr}} \approx 1.5\times 10^{-4} a_{\mathrm{i}}^{1/2}, \quad (5)$$

where a_{dr} and a_{i} are measured in centimeters. The substitution of $a_{\mathrm{i}} = 7.2$ cm into Eq. (5) gives $a_{\mathrm{dr}} \approx 4$ μm.

The velocity of the ejected material at the boundary between zones II and III is given by the expression $u_{mt} = \sqrt{2E_{cmt}} \approx 1.5$ km/s, whereas the velocity of the ejected material at the boundary between zones I and II is $u_v = \sqrt{2E_{cv}} \approx 6$ km/s. Here, $E_{cmt} \approx 1.1$ MJ/kg is the specific threshold internal energy of complete melting of continuous gabbroid anorthosite and $E_{cv} \approx 18$ MJ/kg is the specific threshold internal energy of complete evaporation (under the conditions of fast adiabatic mechanical unloading). Thus, only drops formed in the material melting zone II are ejected by the shock wave from the meteoroid explosion from the surface of the Moon at a high velocity (1.5–6 km/s) and rise to a high altitude. Regolith particles or their fragments from zones III–V have characteristic sizes of about 10–100 μm (the maximum of the size distribution is in the range of 50–70 μm) and rise to lower altitudes at velocities lower than the velocities of droplets.

The dynamics and charging of a dust particle over the Moon are described by the equations [9]

$$m_{\mathrm{d}}\frac{d^2h}{dt^2} = q_{\mathrm{d}}E - m_{\mathrm{d}}g_{\mathrm{M}}, \quad (6)$$

$$\frac{dq_{\mathrm{d}}}{dt} = I_e(q_{\mathrm{d}}) + I_{\mathrm{i}}(q_{\mathrm{d}}) - I_{\mathrm{ph}}(q_{\mathrm{d}}) + I_{e,\mathrm{ph}}(q_{\mathrm{d}}). \quad (7)$$

Here, h is the altitude over the surface of the Moon; m_{d} and q_{d} are the mass and charge of a dust particle, respectively; E is the electric field strength; g_{M} is the gravitational acceleration near the surface of the Moon; $I_e(q_{\mathrm{d}})$ and $I_i(q_{\mathrm{d}})$ are the microscopic currents of electrons and ions of the solar wind to the dust particle, respectively; $I_{\mathrm{ph}}(q_{\mathrm{d}})$ is the photoelectron current from the dust particle caused by its interaction with solar radiation; and $I_{e,\mathrm{ph}}(q_{\mathrm{d}})$ is the photoelectron current to the dust particle. These currents are given by the expressions

$$I_e \approx -\pi a^2 e n_{e\mathrm{S}}\sqrt{\frac{8T_{e\mathrm{S}}}{\pi m_e}}\left(1 + \frac{Z_{\mathrm{d}}e^2}{aT_{e\mathrm{S}}}\right), \quad (8)$$

$$\begin{aligned} I_{\mathrm{i}} \approx{}& \pi a^2 e n_{\mathrm{iS}}\sqrt{\frac{T_{\mathrm{iS}}}{2\pi m_{\mathrm{i}}}}\frac{u_{T\mathrm{i}}}{u_{\mathrm{iS}}} \\ &\times\left\{\frac{u_{\mathrm{iS}} + u_0}{u_{T\mathrm{i}}}\exp\left(-\frac{(u_{\mathrm{iS}} - u_0)^2}{2u_{T\mathrm{i}}^2}\right)\right. \\ &+ \left.\frac{u_{\mathrm{iS}} - u_0}{u_{T\mathrm{i}}}\exp\left(-\frac{(u_{\mathrm{iS}} + u_0)^2}{2u_{T\mathrm{i}}^2}\right)\right\} \\ &+ \pi a^2 e n_{\mathrm{iS}}\sqrt{\frac{T_{\mathrm{iS}}}{4M_{\mathrm{i}}}}\frac{u_{T\mathrm{i}}}{u_{\mathrm{iS}}}\left\{\mathrm{erf}\left(\frac{u_{\mathrm{iS}} + u_0}{\sqrt{2}u_{T\mathrm{i}}}\right)\right. \\ &+ \left.\mathrm{erf}\left(\frac{u_{\mathrm{iS}} - u_0}{\sqrt{2}u_{T\mathrm{i}}}\right)\right\}\left(1 + \frac{2Z_{\mathrm{d}}e^2}{aT_{\mathrm{iS}}} + \frac{u_{\mathrm{iS}}^2}{u_{T\mathrm{i}}^2}\right), \end{aligned} \quad (9)$$

$$I_{\mathrm{ph}} \approx -\pi a^2 e N_0\sqrt{\frac{T_{e,\mathrm{ph}}}{2\pi m_e}}\left(1 + \frac{Z_{\mathrm{d}}e^2}{aT_{e,\mathrm{ph}}}\right)\exp\left(-\frac{Z_{\mathrm{d}}e^2}{aT_{e,\mathrm{ph}}}\right), \quad (10)$$

$$I_{e,\mathrm{ph}} \approx -\pi a^2 e n_{e,\mathrm{ph}}\sqrt{\frac{8T_{e,\mathrm{ph}}}{\pi m_e}}\left(1 + \frac{Z_{\mathrm{d}}e^2}{aT_{e,\mathrm{ph}}}\right). \quad (11)$$

Expressions (8)–(11) are valid for positively charged dust particles. Here, a and Z_{d} are the size and charge number ($q_{\mathrm{d}} = Z_{\mathrm{d}}e$) of a dust particle, respectively; e is the elementary charge; $n_{e(\mathrm{i})\mathrm{S}}$ and $T_{e(\mathrm{i})\mathrm{S}}$ are the density and temperature of electrons (ions) of the solar wind, respectively; m_e and M_{i} are the masses of the electron and ion, respectively; $u_0 = \sqrt{2Z_{\mathrm{d}}e^2/aM_{\mathrm{i}}}$; $u_{T\mathrm{i}} = \sqrt{T_{\mathrm{iS}}/M_{\mathrm{i}}}$ is the thermal velocity of ions of the solar wind; u_{iS} is the velocity of the solar wind; and $n_{e,\mathrm{ph}}$ ($T_{e,\mathrm{ph}}$) is the density (temperature) of photoelectrons from the surfaces of dust particles (it is taken into account that dust particles are located over the dark part of the Moon, but are illuminated by solar light).

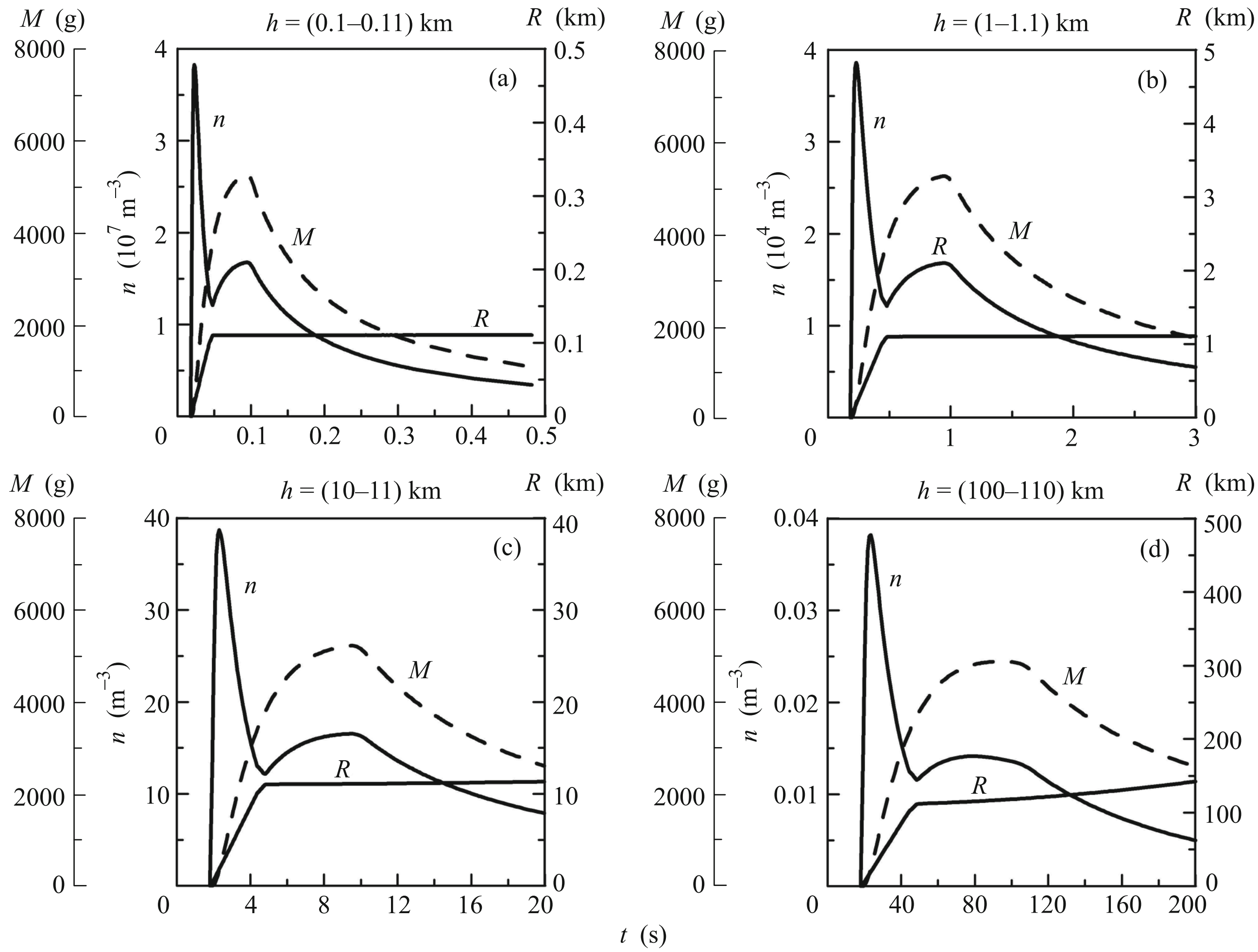

Fig. 2. Dynamics of layers of the dusty plasma cloud formed by solidified melt droplets at the altitudes h = (a) 0.1–0.11, (b) 1–1.1, (c) 10–11, and (d) 100–110 km. Time dependences of (R) the radius characterizing the size of the layer in the direction parallel to the surface subjected to the meteoroid impact, (M) the total mass of dust particles in the layer, and (n) the volume-average dust particle density.

Expression (10) for the current $I_{\rm ph}$ does not include a factor with the characteristics of radiation spectra because the surfaces of dust particles and the surface of the Moon have the same photoelectric properties (work function and quantum yield). In this situation, this factor can be expressed in terms of the photoelectron density N_0 from the illuminated surface of the Moon at $h \to 0$, which depends on the work function and quantum yield of lunar soil [10].

Below, we report the results of calculations for altitudes above 100 m over the surface of the Moon. In this case, the effect of electric fields from the charged surface of the Moon and from neighboring dust particles (in view of their low density) on the dust particle can be neglected. In this situation, dust particles acquire significant charges in quite small times. The charges of particles at altitudes above 100 m are determined primarily by the microscopic current of electrons of the solar wind and by the current of photoelectrons from a dust particle, which is due to its interaction with solar radiation. The magnitudes of these currents hardly depend on the altitude above the surface of the Moon. Consequently, the charges obtained for particles with the same size are the same at different altitudes. For the typical work function $W = 6$ eV and the quantum yield taken from [23], which was experimentally obtained for lunar dust samples delivered to the Earth by the Apollo-14 and Apollo-15 missions, typical parameters are $N_0 = 2.9 \times 10^2$ cm^{-3} and $T_{e,\rm ph} = 1.9$ eV [10]. For these values and the following parameters of the solar wind, $n_{e\rm S} = n_{\rm iS} = 8.7$ cm^{-3}, $T_{e\rm S} = 12$ eV, $T_{\rm iS} = 6$ eV, and $u_{\rm iS} = 4.68 \times 10^5$ cm/s, the charge numbers of particles in the cloud formed by regolith particles (or fragments) reach $Z_{\rm d} \sim 2 \times 10^5$ (for $a \approx 70$ μm) in a time of about 0.5 s. At the same time, particles in the cloud formed by solidified melt

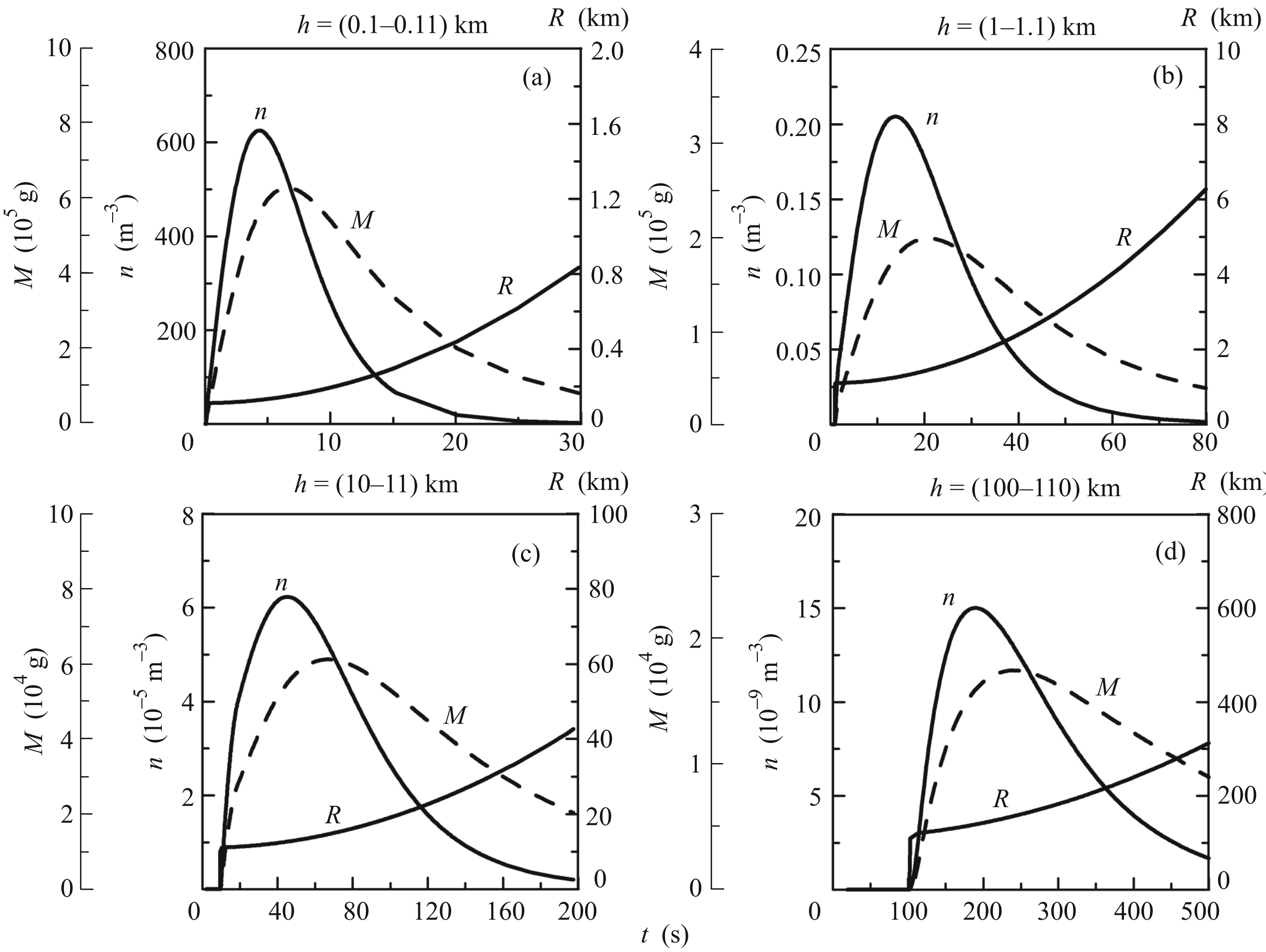

Fig. 3. Dynamics of layers of the dusty plasma cloud formed by particles (or fragments) of regolith at the altitudes h = (a) 0.1–0.11, (b) 1–1.1, (c) 10–11, and (d) 100–110 km. Time dependences of (R) the radius characterizing the size of the layer in the direction parallel to the surface subjected to the meteoroid impact, (M) the total mass of dust particles in the layer, and (n) the volume-average dust particle density.

drops acquire charge numbers of $Z_d \sim 10^4$ in a time of about 10 s. The times of charging of dust particles are much smaller than the evolution times of these clouds. Thus, the expansion of clouds of charged dust particles is observed in the considered situation.

Figures 2 and 3 show the results characterizing the dynamics of different dust layers for the dusty plasma cloud formed by solidified melt drops and that formed by regolith particles (or fragments), respectively.

It is also noteworthy that the mass of the melt ejected from the surface of the Moon into free space by the shock wave from the meteoroid impact is two orders of magnitude smaller than the mass of ejected regolith particles. The number of droplets (several microns in size) into which the melt decays is several orders of magnitude larger than the number of large (several tens of microns in size) ejected regolith particles. Thus, the discussed dusty plasma clouds are strongly different from each other. In the plan view (corresponding to the real observation), these clouds expand in the horizontal plane. The calculated time dependences of the radius R of the cloud characterizing its boundary in the horizontal plane, the altitude $H(R)$ of the boundary of this cloud over the surface of the Moon, and the dust particle density $n(R)$ at this boundary are shown in Fig. 4 (for the cloud formed by solidified melt droplets) and Fig. 5 (for the cloud formed by regolith particles (or fragments)). The data presented in Figs. 4 and 5 allow the determination of the expansion velocities of dust clouds dR/dt. The expansion velocity of the cloud formed by solidified melt droplets appears to be about 2 km/s, whereas the expansion velocity of the cloud formed by regolith particles (or fragments) is about 1 km/s. Correspondingly, the expansion of the cloud of solidified droplets is much faster than that of the cloud of regolith particles. This conclusion is in agreement with the observational data presented in Fig. 1, according to which the expansion velocity of the fast cloud is several kilome-

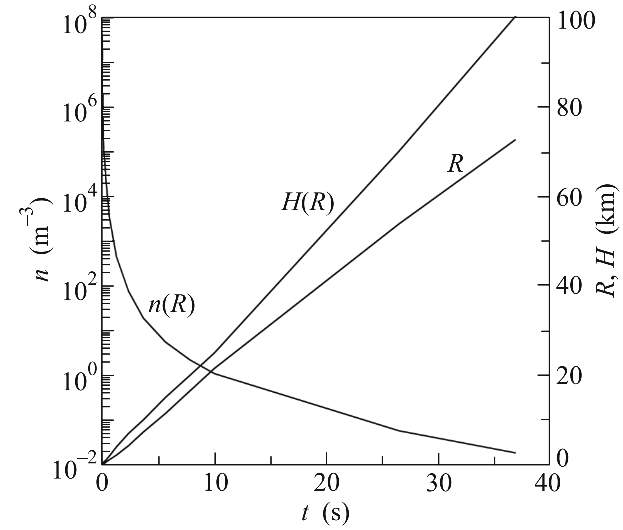

Fig. 4. Time dependences of the radius R of the cloud formed by solidified melt droplets, the altitude $H(R)$ of the boundary of this cloud over the surface of the Moon, and the dust particle density $n(R)$ at the boundary of the cloud.

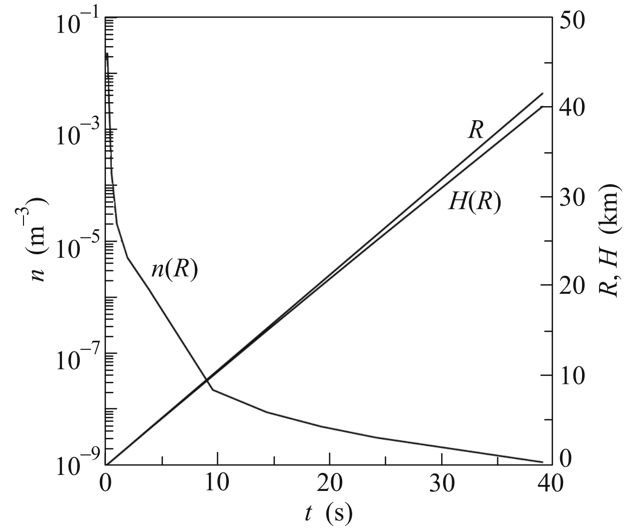

Fig. 5. Time dependences of the radius R of the cloud formed by particles (or fragments) of regolith, the altitude $H(R)$ of the boundary of this cloud over the surface of the Moon, and the dust particle density $n(R)$ at the boundary of the cloud.

ters per second, whereas the expansion velocity of the slow cloud is most probably below 1 km/s.

Calculations similar to those performed in this work but for a minimum energy of 6×10^8 J (from the range of possible kinetic energies of a meteoroid) give quite close expansion velocities of both clouds. This circumstance prevents the observation of two (fast large and slow small) dusty plasma clouds. Thus, the event on February 26, 2015, was apparently induced by a sufficiently large fast meteoroid. We also note that, within the presented theoretical model and for the considered parameters of the materials of the meteoroid and lunar soil, at the velocity of the incident meteoroid below 7.5 km/s, only the material in an unmelted state was ejected from the surface of the Moon by the shock wave. In this case, only one cloud consisting of regolith particles is formed.

The propagation of the dust cloud is accompanied by the appearance of asymmetry with respect to the point (0, 0) (see Fig. 1) because the surface of the Moon is inclined to the horizon. If the meteoroid is incident on the surface of the Moon inclined at the angle α to the horizon, the formed dust cloud expands in the horizontal direction asymmetrically with respect to the point of incidence. In this case, observing the cloud from above, one can identify the maximum $R_{\max}$ and minimum $R_{\min}$ distances from the point of incidence to the boundary of the cloud. These distances can be represented in the form

$$R_{\max} = H(R)\sin\alpha + R\cos\alpha,$$
$$R_{\min} = H(R)\sin\alpha - R\cos\alpha. \quad (12)$$

Here, R is the radius of the boundary of the dust cloud caused by the meteoroid impact on the horizontal surface and $H(R)$ is the altitude of this boundary over the surface of the Moon (see Figs. 4 and 5). The factor of asymmetry was disregarded in the calculations because of the absence of information on the relief of the surface of the Moon in the region unperturbed by the meteoroid impact. In reality, the surface of the Moon can have valleys and hills. Thus, there is a large uncertainty in the angle of ejection of the material with respect to the horizon. For this reason, detailed quantitative agreement between the calculations and observational data should not been expected.

To summarize, we have presented a mechanism explaining the appearance of two dusty plasma clouds because of the meteoroid impact on the surface of the Moon observed on February 26, 2015. The main characteristics of these clouds have been calculated. It has been shown that the shock wave from the meteoroid impact ejects lunar regolith particles (or fragments) and melt from the surface of the Moon into free space. Rising over the surface of the Moon, both regolith particles (or fragments) and melt droplets become electrically charged because of the interaction, in particular, with electrons of the solar wind and with solar radiation. As a result, two dusty plasma clouds appear. The first cloud is formed regolith by particles (or fragments) and the second cloud is formed by solidified melt droplets. These clouds have different characteristics (cloud expansion velocity, total mass of the particles in a cloud, characteristic sizes of the particles in the cloud, number densities and charges of the particles, etc.). Consequently, the clouds can be observed separately. Qualitative agreement has been achieved between the calculated expansion velocities of clouds and observational data. It has been shown that the event observed on February 26, 2015, was most likely induced by a fairly large fast meteoroid with the parameters corresponding to the upper part of the range of possible kinetic energies of meteoroids, which was obtained by calculating the kinetic energy of the impactor from the maximum brightness of the flash. Events similar to that on February 26, 2015, significantly change the properties of the dusty plasma system over the Moon. In particular, a noticeable amount of dust lunar regolith particles (or fragments) with sizes of about 10–100 μm, whose amount in the exosphere is usually small, is ejected into the exosphere of the Moon [14].

This work was supported by the Russian Science Foundation (project no. 17-12-01458).

REFERENCES

1. T. J. Stubbs, R. R. Vondrak, and W. M. Farrell, Adv. Space Res. **37**, 59 (2006).
2. Z. Sternovsky, P. Chamberlin, M. Horányi, S. Robertson, and X. Wang, J. Geophys. Res. **113**, A10104 (2008).
3. T. J. Stubbs, D. A. Glenar, W. M. Farrell, R. R. Vondrak, M. R. Collier, J. S. Halekas, and G. T. Delory, Planet. Space. Sci. **59**, 1659 (2011).
4. A. P. Golub', G. G. Dol'nikov, A. V. Zakharov, L. M. Zelenyi, Yu. N. Izvekova, S. I. Kopnin, and S. I. Popel, JETP Lett. **95**, 182 (2012).
5. E. A. Lisin, V. P. Tarakanov, O. F. Petrov, S. I. Popel', G. G. Dol'nikov, A. V. Zakharov, L. M. Zelenyi, and V. E. Fortov, JETP Lett. **98**, 664 (2013).
6. T. M. Burinskaya, Plasma Phys. Rep. **40**, 14 (2014).
7. S. I. Popel, L. M. Zelenyi, and B. Atamaniuk, Phys. Plasmas **22**, 123701 (2015).
8. S. I. Popel, A. P. Golub', L. M. Zelenyi, and A. Yu. Dubinskii, Planet. Space Sci. **156**, 71 (2018).
9. S. I. Popel, S. I. Kopnin, A. P. Golub', G. G. Dol'nikov, A. V. Zakharov, L. M. Zelenyi, and Yu. N. Izvekova, Solar Syst. Res. **47**, 419 (2013).
10. S. I. Popel, A. P. Golub', Yu. N. Izvekova, V. V. Afonin, G. G. Dol'nikov, A. V. Zakharov, L. M. Zelenyi, E. A. Lisin, and O. F. Petrov, JETP Lett. **99**, 115 (2014).
11. I. A. Kuznetsov, S. L. G. Hess, A. V. Zakharov, F. Cipriani, E. Seran, S. I. Popel, E. A. Lisin, O. F. Petrov, G. G. Dolnikov, A. N. Lyash, and S. I. Kopnin, Planet. Space Sci. **156**, 62 (2018).
12. M. Horányi, Z. Sternovsky, M. Lankton, C. Dumont, S. Gagnard, D. Gathright, E. Grün, D. Hansen, D. James, S. Kempf, B. Lamprecht, R. Srama, J. R. Szalay, and G. Wright, Space Sci. Rev. **185**, 93 (2014).
13. M. Horányi, J. R. Szalay, S. Kempf, J. Schmidt, E. Grün, R. Srama, and Z. Sternovsky, Nature (London, U.K.) **522**, 324 (2015).
14. S. I. Popel, A. P. Golub', E. A. Lisin, Yu. N. Izvekova, B. Atamaniuk, G. G. Dol'nikov, A. V. Zakharov, and L. M. Zelenyi, JETP Lett. **103**, 563 (2016).
15. S. I. Popel, A. P. Golub', L. M. Zelenyi, and M. Horányi, JETP Lett. **105**, 635 (2017).
16. I. V. Nemtchinov, V. V. Shuvalov, N. A. Artemieva, I. B. Kosarev, and S. I. Popel, Int. J. Impact Eng. **27**, 521 (2002).
17. https://www.nasa.gov/centers/marshall/news/lunar/lunar_impacts.html.
18. J. L. Ortiz, J. M. Madiedo, N. Morales, P. Santos-Sanz, and F. J. Aceituno, Mon. Not. R. Astron. Soc. **454**, 344 (2015).
19. H. J. Melosh, *Impact Cratering: A Geologic Process,* Oxford Monographs on Geology and Geophysics (Oxford Univ. Press, Oxford, 1996).
20. J. E. Colwell, S. Batiste, M. Horányi, S. Robertson, and S. Sture, Rev. Geophys. **45**, RG2006 (2007).
21. V. V. Adushkin and A. A. Spivak, *Underground Explosions* (Nauka, Moscow, 2007) [in Russian].
22. H. J. Melosh and A. M. Vickery, Nature (London, U.K.) **350**, 494 (1991).
23. R. F. Willis, M. Anderegg, B. Feuerbacher, and B. Fitton, in *Photon and Particle Interactions with Surfaces in Space,* Ed. by R. J. L. Grard (D. Reidel, Dordrecht, 1973), p. 389.

Translated by R. Tyapaev